ENERGIZED Ca^{2+} TRANSPORT BY HEPATOPANCREATIC BASOLATERAL PLASMA MEMBRANES OF *HOMARUS AMERICANUS*

ZHENPENG ZHUANG AND GREGORY A. AHEARN*

Department of Zoology, 2538 The Mall, University of Hawaii at Manoa, Honolulu, HI 96822, USA

*Author for correspondence (e-mail: ahearn@zoogate.zoo.hawaii.edu)

Summary

Ca^{2+} transport by hepatopancreatic basolateral membrane vesicles of Atlantic lobster (*Homarus americanus*) occurred by at least two independent processes: (1) an ATP-dependent carrier transport system, and (2) a Na$^+$-gradient-dependent carrier mechanism. The sensitivity of ATP-dependent Ca^{2+} transport to vanadate indicated that it was probably due to a P-type ATPase. This system exhibited an extremely high apparent affinity for Ca^{2+} (K_t=65.28±14.39 nmol l^{-1}; J_{max}=1.07±0.06 pmol μg^{-1} protein 8 s^{-1}). The Na$^+$-gradient-dependent carrier transport system exhibited the properties of a Ca^{2+}/Na$^+$ antiporter capable of exchanging external Ca^{2+} with intravesicular Na$^+$ or Li$^+$. Kinetic analysis of the Na$^+$-dependence of the antiport indicated that at least three Na$^+$ were exchanged with each Ca^{2+} (n=2.91±0.22). When Li$^+$ replaced Na$^+$ in exchange for ^{45}Ca^{2+}, the apparent affinity for Ca^{2+} influx was not significantly affected (with Na$^+$, K_t=14.57±5.02 μmol l^{-1}; with Li$^+$, K_t=20.17±6.99 μmol l^{-1}), but the maximal Ca^{2+} transport velocity was reduced by a factor of three (with Na$^+$, J_{max}=2.72±0.23 pmol μg^{-1} protein 8 s^{-1}; with Li$^+$, J_{max}=1.03±0.10 pmol μg^{-1} protein 8 s^{-1}). It is concluded that Ca^{2+} leaves hepatopancreatic epithelial cells across the basolateral membrane by way of a high-affinity, vanadate-sensitive Ca^{2+}-ATPase and by way of a low-affinity Ca^{2+}/Na$^+$ antiporter with an apparent 3:1 exchange stoichiometry. The roles of these transporters in Ca^{2+} balance during the molt cycle are discussed.

Key words: Ca^{2+}, basolateral membrane, BLMV, Ca^{2+}/Na$^+$ antiporter, Ca^{2+}-ATPase, vanadate, antiporter, hepatopancreas, lobster, *Homarus americanus*.

Introduction

Animal studies, largely with vertebrate species, suggest that epithelial Ca^{2+} absorption occurs *via* both an active and a passive pathway (Bronner *et al.* 1986; Favus, 1985; Murer and Hildmann, 1981). The passive process occurs exclusively through the paracellular pathway, while the active step in Ca^{2+} transport is located at the basolateral domain of the enterocytes (Hildmann *et al.* 1982; Nellans and Popovitch, 1981).

The presence of a high-affinity Ca^{2+}-ATPase isolated from basolateral membranes of rat duodenum (Ghijsen *et al.* 1986), jejunum (Nellans and Popovitch, 1981) and kidney (Tsukamoto *et al.* 1986), as well as from plasma membranes of gill epithelia of the crab (*Carcinus maenas*) (Flik *et al.* 1994) and a fish (*Oreochromis mossambicus*) (Flik *et al.* 1993), has been reported. These Ca^{2+} pumps are thought to be involved in Ca^{2+} translocation across the plasma membrane against an unfavorable electrochemical gradient. In addition to the occurrence of this primary active transport system, the presence of a basolateral Ca^{2+}/Na$^+$ exchange process, which may be responsible for a significant portion of Ca^{2+} transport at this cell pole, has been suggested for gill epithelia from crustaceans (Towle, 1993; Flik *et al.* 1994), and it may also be present on the basolateral membrane of rat small intestine and kidney (Hildmann *et al.* 1982; Jayakumar *et al.* 1984; Tsukamoto *et al.* 1986; Van Heeswyk *et al.* 1984).

Our recent studies with lobster (*Homarus americanus*) hepatopancreatic and starfish (*Pycnopodia helianthoides*) pyloric cecal brush-border membrane vesicles indicated that a considerable fraction of the luminal Ca^{2+} content is transported into epithelial cells through a combination of three transport processes: (1) an amiloride-sensitive carrier system; (2) an amiloride-insensitive carrier system; and (3) a potential-sensitive, verapamil- or nifedipine-inhibitable, Ca^{2+} channel (Ahearn and Franco, 1990, 1991, 1993; Zhuang *et al.* 1995; Zhuang and Ahearn, 1996). Little is known about Ca^{2+} transport into the hemolymph across the lobster hepatopancreatic basolateral membrane, with the exception of our preliminary studies suggesting the occurrence of a Ca^{2+}-ATPase and a Ca^{2+}/Na$^+$ antiporter in the basolateral membranes of this crustacean organ (Ahearn and Zhuang, 1996). In the present study, the basolateral Ca^{2+} transport processes of the lobster hepatopancreas are investigated in detail and are discussed in relation to the interplay of basolateral and brush-border Ca^{2+} transport systems during the molt cycle.

Materials and methods

Live Atlantic lobsters (*Homarus americanus* Milne-Edwards; 0.5 kg each) were purchased from commercial dealers in Hawaii and maintained unfed at 10 °C for up to 1 week in filtered sea water. Most animals were in either intermolt or early premolt as assessed by the molt stage classification scheme introduced by Aiken (1973).

Hepatopancreatic basolateral membrane vesicles (BLMVs) were prepared from fresh organs of individual lobsters. BLMVs were prepared freshly for each experiment utilizing a self-orienting Percoll gradient centrifugation technique adapted from a procedure developed for mammals (Davies *et al.* 1987).

Hepatopancreatic tissue was quickly excised and placed into a hypotonic (relative to blood) buffered sucrose medium containing $250 \, \text{mmol} \, l^{-1}$ sucrose, $20 \, \text{mmol} \, l^{-1}$ Tris/HCl, $300 \, \mu \text{mol} \, l^{-1}$ phenylmethylsulfonylfluoride (PMSF), pH 7.4, and homogenized with a Kinematica GmbH polytron. An initial centrifugation at $2500 \, \boldsymbol{g}$ removed large cellular debris. A crude separation of basolateral membranes was obtained from a second centrifugation at $20 \, 400 \, \boldsymbol{g}$. The crude basolateral membrane pellet was resuspended in the hypotonic sucrose buffer, combined with a premixed dilution of Percoll, and centrifuged at $47 \, 800 \, \boldsymbol{g}$ for 1 h. The resulting Percoll-gradient bands were enzymatically assayed for enrichment of the basolateral marker enzyme Na^+/K^+-ATPase and the brush-border membrane marker enzyme alkaline phosphatase. High levels of Na^+/K^+-ATPase enrichment (15.2-fold) and minimal alkaline phosphatase enrichment (1.2-fold) occurred in a band containing a high concentration of BLMVs with minimal contamination by brush-border membrane vesicles (BBMVs; Duerr and Ahearn, 1996).

Vesicle orientation and leakiness were determined by the Na^+/K^+-ATPase latency technique described for this basolateral membrane preparation using a sucrose gradient purification method described previously (Ahearn *et al.* 1987). This method consists of using the asymmetry of ligand binding sites of Na^+/K^+-ATPase in the presence and absence of a detergent to estimate the percentages of right-side-out, inside-out and leaky-sheet membranes in a hepatopancreatic basolateral preparation. Preparing hepatopancreatic basolateral vesicles by a sucrose gradient method resulted in a vesicle preparation that possessed 62.9 % leaky sheets, 31.1 % right-side-out vesicles and 6.0 % inside-out vesicles (Ahearn *et al.* 1987). The same method of assessing vesicle sidedness was applied to the present preparation isolated using Percoll density gradient centifugation. Table 1 indicates that very similar results were obtained for the orientation of vesicles isolated by Percoll. In this instance, 65.24 % of the membranes were leaky sheets, 28.72 % were right-side-out vesicles and 6.04 % were inside-out vesicles. Where capacities between different transport systems are discussed in this paper, appropriate corrections for the orientation of functional vesicles have been considered.

The basolateral membrane fraction was homogenized with inside buffer (compositions varying with experiment, see figure legends for details) and then centrifuged for 40 min at $47 \, 800 \, \boldsymbol{g}$. The resulting pellet was resuspended and washed in

Table 1. *Effects of ouabain and sodium deoxycholate on ATPase activity and associated orientations of lobster hepatopancreatic BLMVs*

Treatment or vesicle orientation	ATPase activity ($\mu \text{mol} \, P_i$ released mg^{-1} protein min^{-1})			
	1	2	3	Mean value
−Ouabain, −DOC	5.38±0.02	5.04±0.04	5.41±0.02	
+Ouabain, −DOC	0.75±0.07	0.80±0.02	0.73±0.03	
−Ouabain, +DOC	7.67±0.12	7.55±0.17	7.50±0.12	
+Ouabain, +DOC	0.43±0.05	0.46±0.08	0.51±0.12	
% Leaky sheets	63.74	66.38	65.61	65.24±0.78
% Right side out	30.54	29.19	26.44	28.72±1.21
% Inside out	5.72	4.43	7.96	6.04±1.03

Values are means ± S.E.M., N=3–5 for each of three different preparations.

fresh intravesicular medium and centrifuged a final time for 40 min at $47 \, 800 \, \boldsymbol{g}$ to collect the pellet.

Long-term and short-term $^{45}\text{Ca}^{2+}$ uptake time-course experiments were conducted in a manner similar to that reported previously (Ahearn *et al.* 1995; Ahearn and Zhuang, 1996; Zhuang and Ahearn, 1996). At the beginning of a transport experiment, a volume (e.g. $20 \, \mu l$) of basolateral membrane vesicles was added to a volume (e.g. $160 \, \mu l$) of radiolabelled medium containing $^{45}\text{Ca}^{2+}$ (ICN Radiochemicals). Following incubation times ranging from 8 s to 60 min, a known volume (e.g. $20 \, \mu l$) of this reaction mixture was withdrawn and plunged into 2 ml of ice-cold stop solution (composition differing with different experiments; see figure legends). The resulting suspensions were rapidly filtered through Millipore filters ($0.65 \, \mu m$ pore diameter) to retain the vesicles and washed with another 5 ml of stop solution. Filters were then added to ICN Ecolume scintillation cocktail and counted for radioactivity in a Beckman LS-8100 scintillation counter. Incubation times and intravesicular media varied for different experiments as indicated in the figure legends. Ca^{2+} uptake values were expressed as pmol per microgram of protein (Bio-Rad protein assay) per filter using the specific activity of $^{45}\text{Ca}^{2+}$ in the incubation medium.

Valinomycin ($50 \, \mu \text{mol} \, l^{-1}$) and bilaterally equal K^+ concentrations across the vesicular wall were present to short-circuit the membranes, and $5 \, \text{mmol} \, l^{-1}$ $MgCl_2$ was used in all ATPase-related experiments. Preliminary experiments have shown that this concentration of ionophore is sufficient to short-circuit the membrane or impose a membrane potential without resulting in significant non-specific transport effects. Each experiment was usually repeated three times using membranes prepared from different animals. Within a given experiment, each point was determined from 3–5 replicate samples. Data are presented as means ± S.E.M. of these replicates in a single representative experiment. Similar qualitative findings were obtained in the repetition of an experiment. Data were analyzed using the computer program SigmaPlot (Jandel), which provides an iterative best fit to experimental values.

Ca^{2+} and Mg^{2+} activity values in external buffers were calculated in all kinetic experiments using the computer program Chelator (Schoenmakers *et al.* 1992) and the chelators EGTA, *N*-hydroxyethyl-EDTA (HEEDTA) and nitrilotriacetic acid (NTA) (0.5 mmol l^{-1} each) taking into account the appropriate pH, temperature and ionic strength of the external media.

^{45}Ca^{2+} was obtained from New England Nuclear Corp., Boston, MA, USA, while reagent grade chemicals valinomycin, tetramethylammonium hydroxide (TMA-OH) and D-gluconic acid lactone were purchased from Sigma Chemical Co., St Louis, USA.

Results

Osmotic reactivity and Ca^{2+} binding properties of lobster hepatopancreatic BLMVs

To determine whether ^{45}Ca^{2+} uptake was into an osmotically active space or represented membrane binding, BLMVs were incubated in outside solutions with various osmolalities provided by using different sucrose concentrations, and ^{45}Ca^{2+} uptake was determined at 15 min (Kikuchi *et al.* 1988). Fig. 1 indicates that a significant ($P<0.01$) linear relationship existed between vesicular ^{45}Ca^{2+} content at 15 min and the reciprocal of the incubation medium osmolality for all membrane preparations. Extrapolation of the curve to the *y*-axis provided an index of non-specific surface ^{45}Ca^{2+} binding to vesicles at 15 min and amounted to approximately 60 % of total ^{45}Ca^{2+}
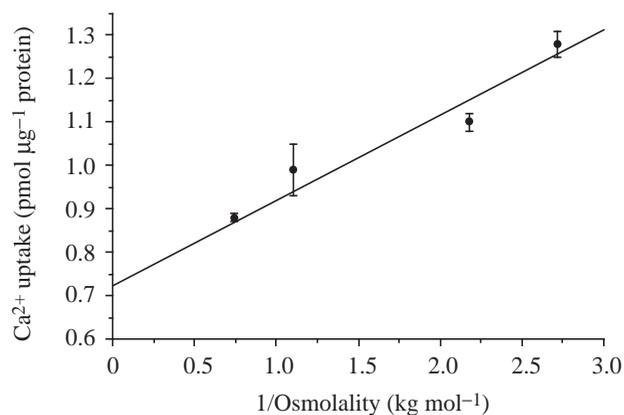

Fig. 1. Effect of transmembrane osmotic gradients on equilibrium uptake of ^{45}Ca^{2+} by basolateral membrane vesicles (BLMVs) of lobster hepatopancreas. Vesicles were loaded with 100 mmol l^{-1} mannitol, 100 mmol l^{-1} KCl, 5 mmol l^{-1} MgCl$_2$, 20 mmol l^{-1} Hepes/Tris at pH 7.0 and were incubated for 90 min in an identical medium containing 0.025 mmol l^{-1} ^{45}Ca^{2+} gluconate and one of the following concentrations of sucrose (in mmol l^{-1}): 800, 500, 100 or 0, providing a series of 1/osmolality values obtained from an osmometer (in kg mol^{-1}): 0.74, 1.10, 2.18 or 2.72, respectively. The line drawn on the figure was computed using linear regression analysis; the values shown are means ± S.E.M., *N*=5 for each mean value. The sample size was four for the regression analysis, r^2=0.94, *P*=0.01).

uptake under control osmotic conditions (0 mmol l^{-1} sucrose) after 15 min of incubation. These results suggest that a significant proportion of the hepatopancreatic BLM preparations were sealed, osmotically reactive and displayed a binding component that had to be taken into account during subsequent influx assessments. A high osmotic sensitivity, with little or no binding of ^{22}Na$^+$ to membrane preparations, has already been reported in a study of ^{22}Na$^+$ uptake by hepatopancreatic BLMVs under the same osmotic conditions as described in the present study (Duerr and Ahearn, 1996). The present results show that considerably more ^{45}Ca^{2+} than ^{22}Na$^+$ tends to bind to hepatopancreatic BLMVs. To correct for non-specific ^{45}Ca^{2+} binding, blanks were prepared during all uptake experiments by exposing membrane preparations and isotope simultaneously to ice-cold stop solution and filtering immediately to collect vesicles for counting of radioactivity. The resulting bound Ca^{2+} was subtracted from total Ca^{2+} uptake at selected exposure intervals to provide estimates of transported Ca^{2+} alone.

Effects of the Ca^{2+} ionophore A23187 and chelator EGTA on Ca^{2+} efflux

Fig. 2 depicts ^{45}Ca^{2+} efflux from preloaded vesicles in the presence of either EGTA alone or EGTA plus Ca^{2+} ionophore A23187. BLMVs were preloaded with ^{45}Ca^{2+} and, after a designated preloading period, a volume of loaded vesicles was
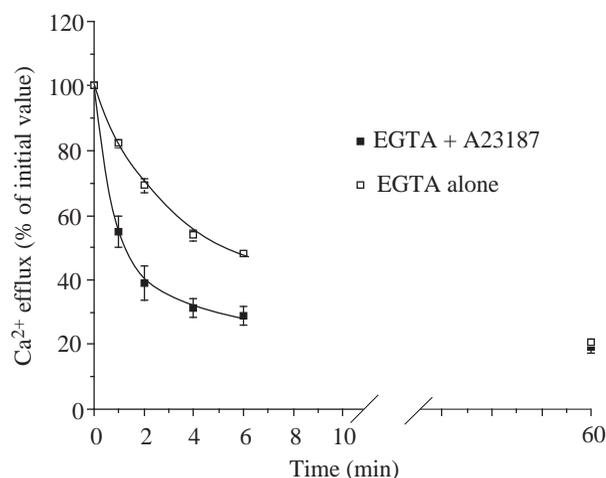

Fig. 2. Effects of 1 mmol l^{-1} EGTA and/or Ca^{2+} ionophore A23187 (20 μmol l^{-1}) on ^{45}Ca^{2+} efflux. Vesicles were loaded with 100 mmol l^{-1} mannitol, 50 mmol l^{-1} sodium gluconate, 50 mmol l^{-1} KCl and 50 μmol l^{-1} valinomycin at pH 7.4 (20 mmol l^{-1} Hepes/Tris). The basolateral membrane vesicles (BLMVs) were then loaded with ^{45}Ca^{2+} by incubating them at the same pH in an outside medium containing 100 mmol l^{-1} mannitol, 50 mmol l^{-1} TMA gluconate, 50 mmol l^{-1} KCl and 0.025 mmol l^{-1} radiolabeled ^{45}Ca^{2+} gluconate. After the incubation, the vesicles were diluted in incubation medium with the same composition as the outside medium but in the presence of either EGTA alone or EGTA plus ionophore A23187. ^{45}Ca^{2+} efflux was determined as a function of time. Data are expressed as a percentage of the initial value at time zero. Bars represent ± S.E.M., *N*=5 for each mean value.
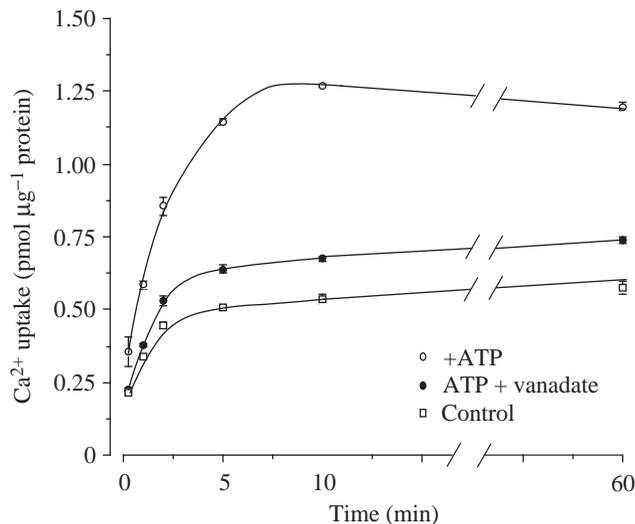
Fig. 3. Effects of external ATP on $^{45}Ca^{2+}$ uptake in short-circuited basolateral membrane vesicles (BLMVs). Vesicles were loaded at pH 7.4 with 100 mmol l^{-1} mannitol, 100 mmol l^{-1} KCl, 5 mmol l^{-1} MgCl$_2$ and 50 μmol l^{-1} valinomycin and were incubated for various times in medium of the same pH with or without 5 mmol l^{-1} Tris/ATP containing 0.025 mmol l^{-1} $^{45}Ca^{2+}$ gluconate, 100 mmol l^{-1} mannitol, 100 mmol l^{-1} KCl and 5 mmol l^{-1} MgCl$_2$. In one case, 0.1 mmol l^{-1} orthovanadate was added to the external medium as an ATP inhibitor. Bars represent ± s.e.m., N=3 for each mean value.

Fig. 4. Effect of pH on ATP-dependent $^{45}Ca^{2+}$ uptake in short-circuited basolateral membrane vesicles (BLMVs). Vesicles were loaded with inside medium containing 100 mmol l^{-1} mannitol, 100 mmol l^{-1} KCl, 5 mmol l^{-1} MgCl$_2$ and 50 μmol l^{-1} valinomycin, at one of three different pH values (pHi), 5.5, 7.4 or 8.0, and each group of vesicles was then incubated for various times with outside medium of the same composition and respective pH (pHe) in the presence of 5 mmol l^{-1} ATP and 0.025 mmol l^{-1} $^{45}Ca^{2+}$ gluconate. Bars represent ± s.e.m., N=3 for each mean value.

removed and diluted in an incubation buffer containing 100 mmol l^{-1} mannitol, 50 mmol l^{-1} TMA gluconate, 50 mmol l^{-1} KCl, 1 mmol l^{-1} EGTA and 20 mmol l^{-1} Hepes/Tris (pH 7.4) with or without 20 μmol l^{-1} (final concentration) A23187. As illustrated in Fig. 2, $^{45}Ca^{2+}$ efflux was significantly accelerated in the presence of A23187 compared with the treatment lacking the ionophore, indicating the presence of $^{45}Ca^{2+}$ within an osmotically reactive intravesicular space.

Occurrence of Ca^{2+}-ATPase in lobster hepatopancreatic BLMVs

To investigate whether Ca^{2+}-ATPase occurred in the hepatopancreatic basolateral membrane preparation, a series of time-course experiments was undertaken. Fig. 3 shows $^{45}Ca^{2+}$ uptake in the presence and absence of 5 mmol l^{-1} ATP, indicating that $^{45}Ca^{2+}$ uptake was significantly greater (P<0.01) in the presence of ATP than in its absence at each time point. The presence of 0.1 mmol l^{-1} vanadate in one group of vesicles with ATP significantly reduced the $^{45}Ca^{2+}$ uptake, providing further evidence that a P-type Ca^{2+}-ATPase occurred in the basolateral membrane of lobster hepatopancreas. It is noteworthy that $^{45}Ca^{2+}$ uptake in the presence of ATP was linear during the first 2 min of incubation and therefore approximated the initial transport rate. A 1 min incubation time was used in subsequent kinetic experiments on Ca^{2+}-ATPase.

To characterize the optimum pH for Ca^{2+}-ATPase in lobster hepatopancreatic BLMVs, buffers at three different pH values were used in one time-course experiment. The results displayed in Fig. 4 suggest that pH 7.4 was near the optimum
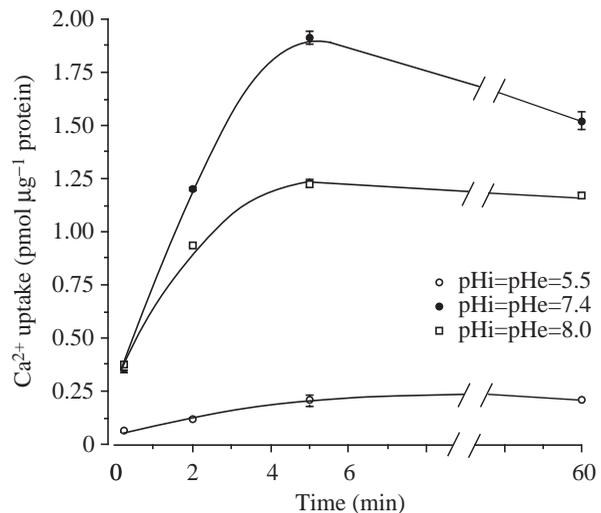
pH in terms of $^{45}Ca^{2+}$ transport, and this value was therefore was chosen for all later experiments concerning Ca^{2+}-ATPase.

Kinetic properties of the Ca^{2+}-ATPase in lobster hepatopancreatic BLMVs

The kinetics of Ca^{2+} influx in hepatopancreatic BLMVs in the presence of 3 mmol l^{-1} ATP is shown in Fig. 5. $^{45}Ca^{2+}$ uptake at 1 min was measured in the presence of different external Ca^{2+} activities (1.38–1419 nmol l^{-1}; activities calculated using total Ca^{2+} concentrations in external media and the Chelator program discussed above). Data are presented in Fig. 5 for an 8 s exposure for comparison with later influx experiments in the absence of ATP. Over the selected activity range, ATP-dependent Ca^{2+} influx was a hyperbolic function of external Ca^{2+} activity, suggesting the presence of a saturable carrier system, which can be described by the Michaelis–Menten equation:

$$J = (J_{max} \times [Ca^{2+}]_o)/(K_t + [Ca^{2+}]_o),   (1)$$

where J is the total $^{45}Ca^{2+}$ influx in pmol μg^{-1} protein 8 s^{-1}, J_{max} is the apparent maximal carrier-mediated influx, K_t (in nmol l^{-1}) is the apparent Ca^{2+} activity resulting in half-maximal influx, and $[Ca^{2+}]_o$ is the external Ca^{2+} activity determined for each total Ca^{2+} concentration using Chelator.

A nonlinear, iterative, best-fit computer program using equation 1 was employed to analyze the data in Fig. 5. Apparent kinetic parameters for the ATP-dependent carrier process calculated in this manner were J_{max}= 1.07±0.06 pmol μg^{-1} protein 8 s^{-1}; K_t=65.28±4.39 nmol l^{-1}.
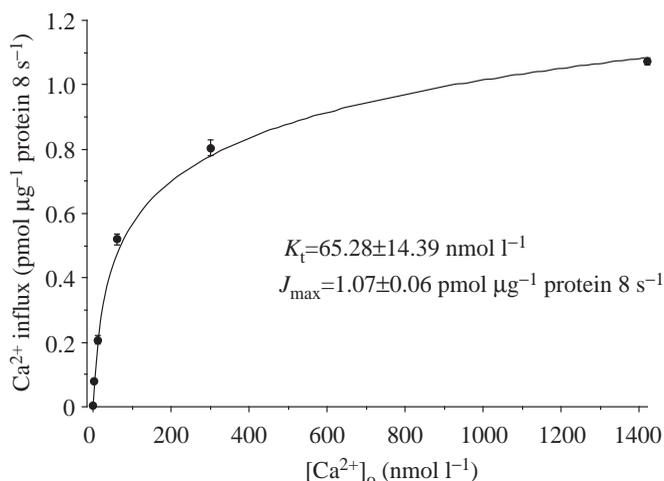
Fig. 5. Kinetics of hepatopancreatic basolateral Ca²⁺-ATPase. Vesicles were loaded with $150\,mmol\,l^{-1}$ KCl, $20\,mmol\,l^{-1}$ Hepes/Tris, $3.34\,mmol\,l^{-1}$ MgCl$_2$ ($0.8\,mmol\,l^{-1}$ free Mg²⁺), $3\,mmol\,l^{-1}$ Tris/ATP, $0.5\,mmol\,l^{-1}$ HEEDTA, $0.5\,mmol\,l^{-1}$ NTA and $0.5\,mmol\,l^{-1}$ EGTA at pH 7.4. These preloaded vesicles were then incubated for 1 min in external medium containing the same constituents as those included within the vesicles except for the addition of various concentrations of ⁴⁵Ca²⁺ gluconate (with Ca²⁺ activities of $1.38–1419\,nmol\,l^{-1}$). Values have been corrected for non-specific Ca²⁺ binding as discussed in the text and are presented as means ± S.E.M. ($N=5$).

Occurrence of Ca²⁺/Na⁺ exchange and the effects of membrane potential on Ca²⁺/Na⁺ exchange in hepatopancreatic BLMVs

The possible presence of a Ca²⁺/Na⁺ antiporter in hepatopancreatic BLMVs was investigated in a time-course experiment using short-circuited vesicles that had been preloaded with Na⁺ or H⁺, providing outwardly directed Na⁺ and H⁺ gradients. The data shown in Fig. 6 indicate that ⁴⁵Ca²⁺ uptake in vesicles with such a Na⁺ gradient was significantly greater than in vesicles without a Na⁺ gradient or in vesicles with an outwardly directed H⁺ gradient. This 'overshoot phenomenon' under these conditions suggests the occurrence of a carrier system that can transiently transport Ca²⁺ against a concentration gradient using energy inherent in the outwardly directed Na⁺ gradient.

Fig. 7 illustrates an experiment to clarify the specificity of the Na⁺-gradient-dependent ⁴⁵Ca²⁺ uptake process. In this experiment, the uptake of ⁴⁵Ca²⁺ by vesicles with outwardly directed Na⁺ or Li⁺ gradients was determined at 15 s and at 6 min intervals. The results of this experiment show that the Ca²⁺/Na⁺ antiporter clearly demonstrated a preference for Na⁺ as an internal exchangeable substrate over Li⁺. Diltiazem, a known inhibitor of Ca²⁺/Na⁺ exchange in mitochondrial membranes (Gunter *et al.* 1994), was ineffective against the antiporter in hepatopancreatic BLMVs (Fig. 7), suggesting a possible fundamental difference between the cation exchangers in the two cellular locations.

Fig. 8 describes the effects of an imposed transmembrane potential (inside negative or positive; K⁺/valinomycin) on Na⁺-

gradient-dependent ⁴⁵Ca²⁺ uptake in hepatopancreatic BLMVs. Fig. 8 indicates that an inside-negative vesicular membrane potential reduced the stimulatory effects of a Na⁺ gradient in terms of ⁴⁵Ca²⁺ uptake, while an inside-positive membrane potential enhanced the effect of the Na⁺ gradient. These results strongly suggest that an electrogenic process is responsible for the exchange of ⁴⁵Ca²⁺ with Na⁺.

Kinetic properties of Ca²⁺/Na⁺ exchange in lobster hepatopancreatic BLMVs

Preliminary ⁴⁵Ca²⁺ uptake experiments with hepatopancreatic BLMVs using exposure intervals of 1–15 s (data not shown) suggested that initial rates of ⁴⁵Ca²⁺/Na⁺ exchange could be approximated using an exposure interval of 8 s. ⁴⁵Ca²⁺ influx in BLMVs was measured as a function of external ⁴⁵Ca²⁺ activity ($12.5\,nmol\,l^{-1}$ to $180\,\mu mol\,l^{-1}$) in the presence of an outwardly directed Na⁺ or Li⁺ gradient, and the results are displayed in Fig. 9. All influx values were corrected for non-specific binding, as reported previously.

As shown in Fig. 9, ⁴⁵Ca²⁺ influxes into vesicles preloaded with either intravesicular Na⁺ or Li⁺ were both hyperbolic functions of external Ca²⁺ activity, possessing rates that could be described by equation 1. Michaelis–Menten constants for vesicles preloaded with Na⁺ were $K_t=14.57\pm5.02\,\mu mol\,l^{-1}$ and $J_{max}=2.72\pm0.23\,pmol\,\mu g^{-1}\,protein\,8\,s^{-1}$. Constants determined
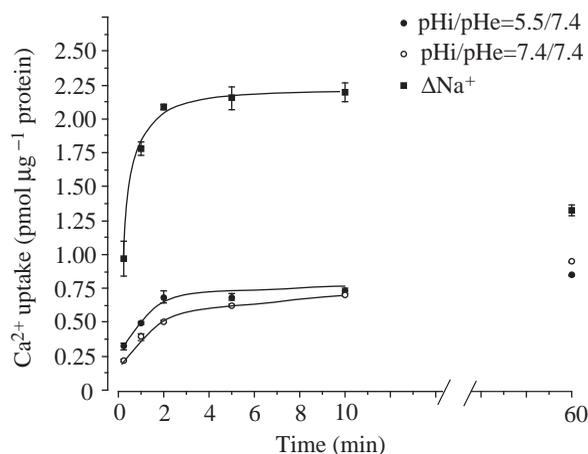

Fig. 6. Effects of outwardly directed pH (pHi/pHe) or Na⁺ (ΔNa⁺) gradients on ⁴⁵Ca²⁺ uptake in short-circuited basolateral membrane vesicles (BLMVs). Vesicles were divided into three groups. One group was loaded at pH 7.4 ($20\,mmol\,l^{-1}$ Hepes/Tris) with inside medium containing $100\,mmol\,l^{-1}$ mannitol, $100\,mmol\,l^{-1}$ KCl and $50\,\mu mol\,l^{-1}$ valinomycin, and was incubated at pH 7.4 in outside medium of the same composition but containing $0.05\,mmol\,l^{-1}$ ⁴⁵Ca²⁺ gluconate. Another was loaded at pH 5.5 ($20\,mmol\,l^{-1}$ Mes/Tris) as above and was incubated at pH 7.4 ($20\,mmol\,l^{-1}$ Hepes/Tris) in outside medium of the same composition, but containing $0.05\,mmol\,l^{-1}$ ⁴⁵Ca²⁺ gluconate. The third group was loaded at pH 7.4 with $100\,mmol\,l^{-1}$ mannitol, $50\,mmol\,l^{-1}$ KCl, $50\,mmol\,l^{-1}$ sodium gluconate and $50\,\mu mol\,l^{-1}$ valinomycin, and was incubated at the same pH in outside medium containing $200\,mmol\,l^{-1}$ mannitol, $50\,mmol\,l^{-1}$ KCl and $0.05\,mmol\,l^{-1}$ ⁴⁵Ca²⁺ gluconate. Values are means ± S.E.M., $N=3$ for each mean value.
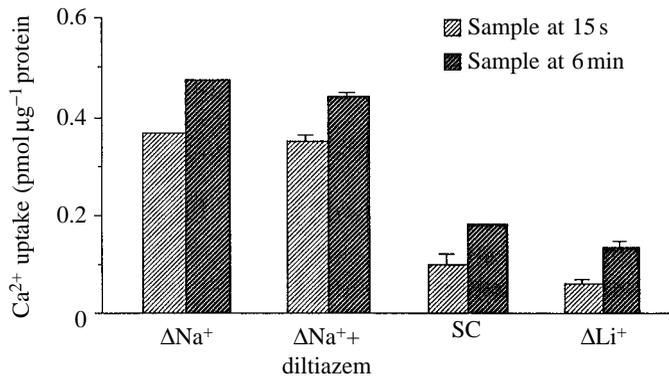
Fig. 7. Effects of outwardly directed Li$^+$ (ΔLi$^+$) or Na$^+$ (ΔNa$^+$) gradients and external diltiazem on ^{45}Ca^{2+}/Na$^+$ exchange in short-circuited basolateral membrane vesicles (BLMVs). Vesicles were divided into three groups. One group was loaded at pH 7.4 (20 mmol l^{-1} Hepes/Tris) with 100 mmol l^{-1} mannitol, 50 mmol l^{-1} KCl, 50 mmol l^{-1} NaCl and 50 μmol l^{-1} valinomycin, and was incubated at pH 7.4 in outside medium of the same composition but containing 50 mmol l^{-1} choline chloride instead of 50 mmol l^{-1} NaCl and 0.05 mmol l^{-1} ^{45}Ca^{2+} gluconate (ΔNa$^+$) in the absence or presence of 1 mmol l^{-1} diltiazem. Another was loaded at pH 7.4 (20 mmol l^{-1} Hepes/Tris) with 100 mmol l^{-1} mannitol, 50 mmol l^{-1} KCl, 50 mmol l^{-1} LiCl and 50 μmol l^{-1} valinomycin, and was incubated at the same pH in the same outside medium as the control group (ΔLi$^+$). The third group was loaded with the same inside medium as the control group and incubated in outside buffer with the same composition as the inside medium, leading to a short-circuited (SC) condition. Values are means + S.E.M., N=5 for each mean value.

for vesicles preloaded with Li$^+$ were K_t=20.17±6.99 μmol l^{-1} and J_{max}=1.03±0.10 pmol μg^{-1} protein 8 s^{-1}. These results suggest that both internal cations could support the exchange process with external Ca^{2+}, but that the maximal transport velocity was three times greater with Na$^+$ than with Li$^+$. There was no apparent difference between the effects of the two preloaded cations on ^{45}Ca^{2+} binding to the external membrane surface (e.g. K_t).

Apparent stoichiometry of ^{45}Ca^{2+}/Na$^+$ exchange

The experiments in Fig. 8 suggested that the ^{45}Ca^{2+}/Na$^+$ exchange process of hepatopancreatic BLMVs was electrogenic, with more positive charge being exchanged in one direction than in the other. To estimate the stoichiometry of the exchange process, ^{45}Ca^{2+} influx (at a fixed external Ca^{2+} activity; 5 μmol l^{-1}) was measured as a function of intravesicular Na$^+$ concentration (0, 5, 10, 20, 35 and 75 mmol l^{-1}). The results shown in Fig. 10 indicate that a sigmoidal relationship existed between the variables according to the Hill equation:

$$J = J_{max}[Na^+]^n/(K_t)^n + [Na^+]^n, \qquad (2)$$

where J_{max} is maximal ^{45}Ca^{2+} influx, $(K_t)^n$ is an affinity constant modified to accommodate multisite interactions (interaction coefficient) and the Hill coefficient n is an estimate of the number of reactive Na$^+$ binding sites on the internal
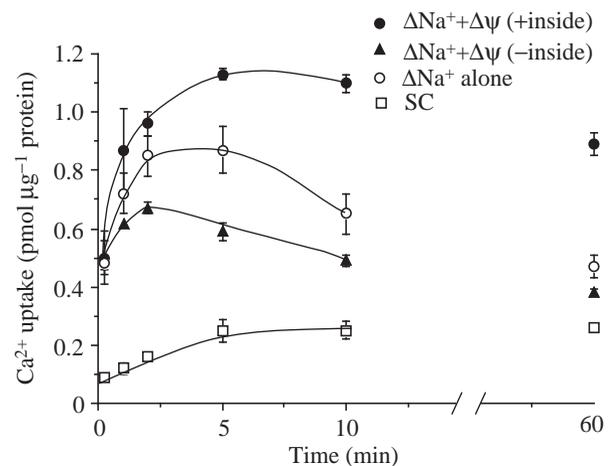

Fig. 8. Effect of membrane potential on 0.05 mmol l^{-1} ^{45}Ca^{2+} uptake in the presence of an outwardly directed Na$^+$ gradient (ΔNa$^+$) by hepatopancreatic basolateral membrane vesicles (BLMVs). Vesicles were loaded with either 50 mmol l^{-1} potassium gluconate or 50 mmol l^{-1} TMA gluconate, 50 mmol l^{-1} sodium gluconate, 100 mmol l^{-1} mannitol and 50 μmol l^{-1} valinomycin at pH 7.5 (25 mmol l^{-1} Hepes/Tris). One group of vesicles was then incubated in medium of the same pH containing 0.05 mmol l^{-1} ^{45}Ca^{2+} gluconate, 50 mmol l^{-1} sodium gluconate and 50 mmol l^{-1} potassium gluconate to produce a short-circuited condition (SC). The second group was incubated at the same pH in outside buffer containing 0.05 mmol l^{-1} ^{45}Ca^{2+} gluconate, 200 mmol l^{-1} mannitol and 50 mmol l^{-1} potassium gluconate to produce an outwardly directed Na$^+$ gradient only (ΔNa$^+$ alone). The last two groups were incubated in outside buffer containing 200 mmol l^{-1} mannitol and 50 mmol l^{-1} TMA gluconate or 50 mmol l^{-1} potassium gluconate to produce imposed membrane potential conditions ($\Delta\psi$, negative or positive inside relative to outside, respectively). Values are means ± S.E.M., N=3 for each mean value.

vesicular surface. The positive vertical axis intercept of Fig. 10 at 0 mmol l^{-1} Na$^+$ suggests the occurrence of a Na$^+$-independent Ca^{2+} uptake process such as diffusion under these conditions. The SigmaPlot curve-fitting program was used to obtain estimates for the three kinetic parameters using equation 2. The best-fitting curve provided the following values for these constants: J_{max}=1.40±0.02 pmol μg^{-1} protein 8 s^{-1}; $(K_t)^n$=10.34±0.29 mmol l^{-1}; and n=2.91±0.22. These results, and those of the electrogenic experiment shown in Fig. 8, suggest that this cation antiporter has an exchange stoichiometry of at least 1Ca^{2+}/3Na$^+$.

Discussion

The present study focuses upon the characterization of Ca^{2+} transport mechanisms of the lobster hepatopancreatic epithelial basolateral membrane. This membrane was prepared using a Percoll gradient centrifugation technique that produced sealed, osmotically reactive vesicles (Figs 1, 2; Table 1). These results, together with the occurrence of an 'overshoot phenomenon' in time-course Ca^{2+} uptake experiments (Fig. 6), suggest that the Ca^{2+} uptake values reported in this study represent transport processes rather than non-specific binding.
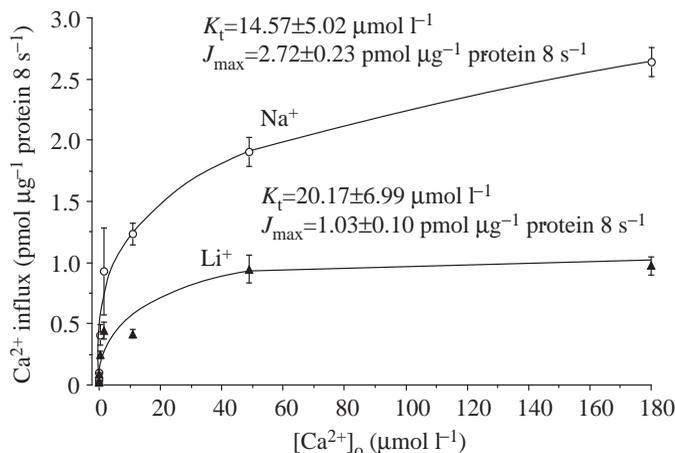
Fig. 9. $^{45}Ca^{2+}$ influx kinetics (8 s uptakes) into hepatopancreatic basolateral membrane vesicles (BLMVs) in the presence of an outwardly directed Na^+ or Li^+ gradient. Vesicles were loaded with 150 mmol l⁻¹ NaCl or 150 mmol l⁻¹ LiCl, 20 mmol l⁻¹ Hepes/Tris, 0.5 mmol l⁻¹ HEEDTA, 0.5 mmol l⁻¹ NTA, 0.5 mmol l⁻¹ EGTA, at pH 7.4, and were then incubated in medium at pH 7.4 containing 150 mmol l⁻¹ KCl, 20 mmol l⁻¹ Hepes/Tris, 0.5 mmol l⁻¹ HEEDTA, 0.5 mmol l⁻¹ NTA, 0.5 mmol l⁻¹ EGTA and various $^{45}Ca^{2+}$ gluconate concentrations (12.5 nmol l⁻¹ to 180 µmol l⁻¹ Ca^{2+} activities). Each influx value was corrected for non-specific binding as discussed in the text. Values are means ± S.E.M., $N=5$ for each mean value.

Fig. 10. Na^+ dependency of $^{45}Ca^{2+}/Na^+$ exchange. Basolateral membrane vesicles (BLMVs) were loaded with 0, 5, 20, 20, 35 or 75 mmol l⁻¹ NaCl (KCl substituting for NaCl to 150 mmol l⁻¹), 20 mmol l⁻¹ Hepes/Tris, 0.5 mmol l⁻¹ HEEDTA, 0.5 mmol l⁻¹ NTA and 0.5 mmol l⁻¹ EGTA at pH 7.4. Preloaded vesicles were then exposed for 8 s to external medium containing 5 µmol l⁻¹ $^{45}Ca^{2+}$ gluconate (Ca^{2+} activity), 150 mmol l⁻¹ KCl, 20 mmol l⁻¹ Hepes/Tris, 0.5 mmol l⁻¹ HEEDTA, 0.5 mmol l⁻¹ NTA and 0.5 mmol l⁻¹ EGTA at pH 7.4. Each influx value was corrected for non-specific isotope uptake as discussed in the text. Values are means ± S.E.M., $N=5$ for each mean value.

Data from basolateral vesicle orientation experiments resulting from a Percoll isolation procedure (Table 1) confirmed the previously reported distribution of leaky sheets, right-side-out vesicles and inside-out vesicles generated using a sucrose gradient (Ahearn *et al.* 1987) and suggested that five times more sealed vesicles were oriented right-side-out than in the other direction.

Sea water contains approximately 10 mmol l⁻¹ Ca^{2+}, and it has been reported that lobsters (*Homarus americanus*) drink a considerable volume of sea water. In addition, they may consume much or all of their old exoskeleton during the process of molting (Mykles, 1980). A significant amount of Ca^{2+} is therefore available to crustacean hepatopancreatic epithelial cells during ecdysis, and this ion is also probably a component of the stomach contents and the hepatopancreatic ducts during normal feeding activities in intermolt. Our previously reported results (Ahearn and Zhuang, 1996; Zhuang and Ahearn, 1996) suggest that Ca^{2+} influx into lobster hepatopancreatic brush-border membrane vesicles occurs by a combination of three transport processes: (1) an amiloride-sensitive carrier system; (2) an amiloride-insensitive carrier system; and (3) a verapamil-inhibited, potential-dependent ion channel. Similar findings were also reported for Ca^{2+} transport by apical membrane vesicles of the kidneys in the same animal, suggesting a common physiological theme for regulating the transmembrane flow of this divalent cation by marine crustacean epithelia (Ahearn and Franco, 1993). It is critical for a crustacean to harden its exoskeleton rapidly during the post-molt stage. Therefore, efficient hepatopancreatic basolateral mechanisms are essential to translocate Ca^{2+} from
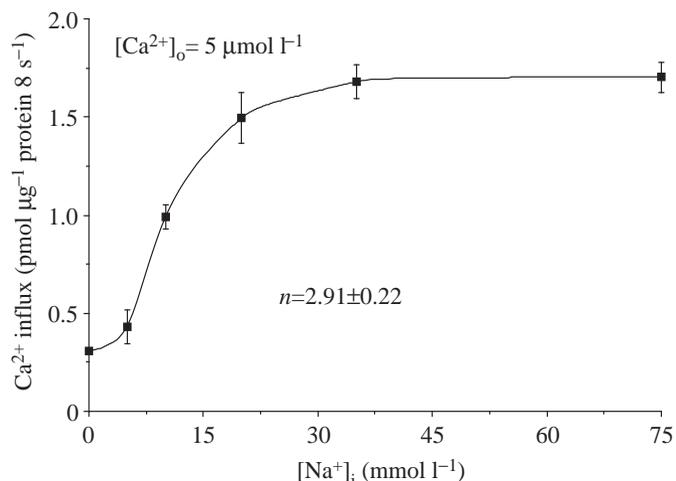
their sequestration sites, such as foregut gastroliths and hepatopancreatic R-cell organelle concretions, to the blood where it is needed for exoskeletal hardening.

Our previously reported preliminary results and the data from the present investigation suggest that Ca^{2+} efflux from lobster hepatopancreatic basolateral membrane vesicles occurred by a combination of two carrier-mediated transport processes: (1) a high-affinity, vanadate-sensitive, ATP-dependent Ca^{2+}-ATPase ($K_t=65.28$ nmol l⁻¹); and (2) a low-affinity, electrogenic $1Ca^{2+}/3Na^+$ antiporter system ($K_t=14.57$ µmol l⁻¹). These mechanisms generally resemble those previously described for crab gill basolateral membranes (Towle, 1993; Flik *et al.* 1994). A quantitative comparison between the carrier-mediated Ca^{2+} efflux kinetic constants for the lobster hepatopancreatic basolateral membrane and those from crab gill, fish gill, fish intestine and rat kidney are displayed in Table 2. Comparison of the values from the five types of animals shown in this table suggests that, while the apparent affinity constant for the lobster Ca^{2+}-ATPase is well within the range described for other tissues, the affinity constant for the electrogenic $1Ca^{2+}/3Na^+$ antiporter is considerably greater than the other values reported for vertebrates and invertebrates. The markedly low apparent affinity of the hepatopancreatic basolateral membrane may relate to the role of this tissue in Ca^{2+} sequestration during the molt cycle. Hepatopancreatic R-cells are known to sequester significant concentrations of Ca^{2+} during premolt when this ion is released from the old exoskeleton and enters the blood. Ca^{2+} is also stored in stomach gastroliths and must pass through the
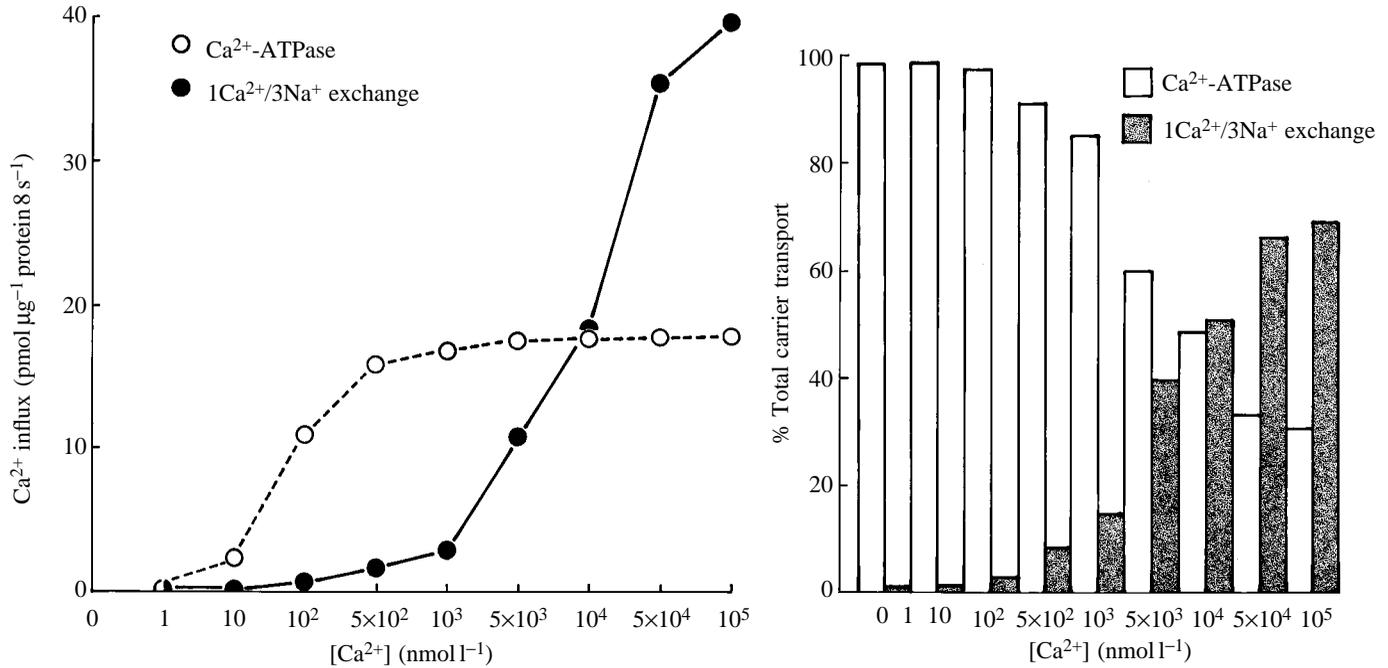
Fig. 11. Relative roles of the Ca^{2+}-ATPase and the electrogenic $1Ca^{2+}/3Na^+$ antiporter in Ca^{2+} transport across lobster hepatopancreatic basolateral membranes over a wide intracellular Ca^{2+} activity range such as might occur during the intermolt, premolt and postmolt stages of the molt cycle. Values in both panels were derived using the kinetic constants derived in the present study for each carrier system and the percentage protein associated with only the inside-out sealed basolateral membrane vesicles (6%) (see Table 1). Under these conditions, J_{max} values in Table 2 become modified to $17.83\,\mathrm{pmol\,\mu g^{-1}\,protein\,8\,s^{-1}}$ for the Ca^{2+}-ATPase and $45.33\,\mathrm{pmol\,\mu g^{-1}\,protein\,8\,s^{-1}}$ for the $1Ca^{2+}/3Na^+$ exchanger.

hepatopancreatic epithelium to reach this latter stomach storage depot. After the molt, the new exoskeleton must be recalcified by the Ca^{2+} kept in the sequestration sites, and transfer of Ca^{2+} occurs through the hepatopancreatic epithelium to the blood. The low apparent affinity of the hepatopancreatic basolateral electrogenic antiporter may be an adaptation of the cell to its role in molting, enabling it to regulate larger swings in intracellular Ca^{2+} activity than those that occur in similar epithelial cells from crustacean gills or vertebrate gut and renal tissues.

Fig. 11 is a comparison of the transporting roles of the lobster hepatopancreatic basolateral Ca^{2+}-ATPase and the electrogenic $1Ca^{2+}/3Na^+$ antiporter at intracellular Ca^{2+} activities between 1 and $100\,000\,\mathrm{nmol\,l^{-1}}$ calculated using apparent K_t and J_{max} values obtained from this study (Table 2), with the maximal transport rates being modified under the assumption that only the protein associated with inside-out vesicles was responsible for Ca^{2+} transport by the Ca^{2+}-ATPase and the $1Ca^{2+}/3Na^+$ antiporter. This assumption is justified for the ATPase because it is assumed that ATP can only gain access to its binding site from the cytoplasmic membrane surface. In the absence of other driving forces, the

Table 2. *Kinetic constants for epithelial basolateral Ca^{2+} transport*

Species and tissue	Ca²⁺-ATPase		Ca²⁺/Na⁺ exchanger		
	K_t (nmol l⁻¹)	J_{max} (pmol mg⁻¹ protein 8 s⁻¹)	K_t (nmol l⁻¹)	J_{max} (pmol μg⁻¹ protein 8 s⁻¹)	Reference
Lobster hepatopancreas (*Homarus americanus*)	65	1.07	14 570	2.72	Present study
Seawater-adapted fish gill (*Oreochromis mossambicus*)	495	0.91	1880	2.08	Verbost *et al.* (1994)
Crab gill (*Carcinus maenas*)	149	0.23	1780	1.32	Flik *et al.* (1994)
Fish intestine (*Oreochromis mossambicus*)	27	0.08	181	0.96	Flik *et al.* (1990)
Rat kidney cortex	110	10.80	200	0.43	van Heeswijk *et al.* (1984)

All temperatures were 25 °C, except for kidney data at 37 °C.

external addition of ATP would only stimulate transport by inside-out vesicles. The asymmetric binding properties of the antiporter similarly justify the hypothesis that only inside-out vesicles are responsible for the exchange properties of Na^+-loaded vesicles. Similar reasoning has been applied to Ca^{2+} transport by the ATPase and antiporter of the intestinal epithelium of the fish *Oreochromis mossambicus* by Schoenmakers and Flik (1992). While crustacean and fish epithelia may differ quantitatively in the relative amounts of Ca^{2+} transferred by each protein, the qualitative roles of inside-out and right-side-out vesicles in Ca^{2+} movements in these two species are probably similar.

Given the above assumptions and caveats concerning vesicle orientation, Fig. 11 suggests that, at intracellular Ca^{2+} activities that might occur in typical epithelial cells (e.g. $100–500\,\mathrm{nmol\,l^{-1}}$), more than 90% of Ca^{2+} efflux takes place by way of the Ca^{2+}-ATPase. Between 1000 and $10\,000\,\mathrm{nmol\,l^{-1}}$, the range of intracellular activities that might occur during temporary Ca^{2+} storage or transcellular Ca^{2+} movements taking place at certain times in the molt cycle, the electrogenic $1Ca^{2+}/3Na^+$ exchanger assumes a greater role in moving the divalent cation out of the cell. In Fig. 11, the crossover point (where efflux by both processes is approximately equal) is $10\,000\,\mathrm{nmol\,l^{-1}}$ (a value near the apparent K_t for the exchanger). Flick *et al.* (1994) described Ca^{2+} efflux by these two transporters in crab gill epithelia and found a crossover point at $500\,\mathrm{nmol\,l^{-1}}$, considerably below that of the hepatopancreas. These results suggest that this crossover point may have biological relevance to the roles the different cell types play in Ca^{2+} balance in the two animals. Because the gills are unlikely to store a large amount of Ca^{2+} or to move massive quantities of this cation to and from sites of sequestration, and because their maximal transport capacities are lower than those of the hepatopancreas (Table 2), it can be assumed that the gill cells may experience smaller fluctuations in intracellular Ca^{2+} activity than those of the hepatopancreas and therefore do not biologically require as high a crossover point as do the cells of the hepatopancreas. From this reasoning, it is likely that in hepatopancreas the Ca^{2+}-ATPase probably serves a housekeeping role by maintaining relatively low intracellular Ca^{2+} levels during intermolt when the animal feeds. However, during molting, when massive Ca^{2+} movements occur into and through this epithelium, the low-affinity, electrogenic $1Ca^{2+}/3Na^+$ exchanger may assume a more significant role in accommodating the increased intracellular Ca^{2+} activity that results.

Data from the present investigation with intermolt lobsters provide tentative clues about how the membrane proteins of the hepatopancreatic brush-border and basolateral membranes may be involved in transcellular Ca^{2+} movements during different molt stages. During the intermolt or feeding stage, the previously reported (Ahearn, 1996; Ahearn and Zhuang, 1996) brush-border amiloride-sensitive carrier system (i.e. an electrogenic $2Na^+/1H^+$ antiporter) may play a major role in Ca^{2+} absorption from the diet into epithelial cells, followed by

Ca^{2+} efflux into the blood through the Ca^{2+}-ATPase and $1Ca^{2+}/3\,Na^+$ antiporter in the basolateral membranes. During the premolt stage, some physiological processes are highly activated to store Ca^{2+} solubilized from the old exoskeleton. Hepatopancreatic epithelial cells probably participate in these processes by upregulating presently undescribed basolateral Ca^{2+} uptake mechanisms from the blood (e.g. putative Ca^{2+} channels or carrier processes) so that Ca^{2+} can then flow efficiently down its electrochemical gradient into the epithelial cells. Some of this Ca^{2+} may be sequestered into mitochondria or other organelles, and the rest is transported out of the cell through the brush border by the amiloride-insensitive carrier system for sequestration by the gastroliths in the stomach. Following ecdysis, an increase in Ca^{2+} concentration in the stomach due to the solubilization of Ca^{2+} from the gastroliths may trigger the opening of the previously described Ca^{2+} channels in the brush-border membrane, which combine with Ca^{2+} uptake by the amiloride-sensitive carrier system to accelerate Ca^{2+} translocation from lumen to cell. Within the cell, the mitochondria and other organelles may release stored Ca^{2+}, which joins with entering gastrolith Ca^{2+} to be transported to the blood by way of the Ca^{2+}-ATPase and $1Ca^{2+}/3Na^+$ antiporter in order to harden the new exoskeleton. Clearly, considerably more work needs to be undertaken to complete this tentative picture of the role of the hepatopancreas in Ca^{2+} balance, but the present study represents a significant step towards our understanding of the cellular mechanisms regulating the massive transcellular Ca^{2+} movements that accompany the growth processes of crustaceans.

References

AHEARN, G. A. (1996). The invertebrate electrogenic $2Na^+/1H^+$ exchanger: Polyfunctional epithelial workstation. *News physiol. Sci.* **11**, 31–35.

AHEARN, G. A. AND FRANCO, P. (1990). Sodium and calcium share the electrogenic $2\,Na^+/1\,H^+$ antiporter in crustacean antennal glands. *Am. J. Physiol.* **259**, F758–F767.

AHEARN, G. A. AND FRANCO, P. (1991). Electrogenic $2Na^+/1H^+$ antiport in echinoderm gastrointestinal epithelium. *J. exp. Biol.* **158**, 495–507.

AHEARN, G. A. AND FRANCO, P. (1993). Ca^{2+} transport pathway in brush border membrane vesicles of crustacean antennal glands. *Am. J. Physiol.* **264**, R1206–R1213.

AHEARN, G. A., GROVER, M. L., TSUJI, R. T. AND CLAY, L. P. (1987). Proton-stimulated $Cl–HCO_3$ antiport by basolateral membrane vesicles of lobster hepatopancreas. *Am. J. Physiol.* **252**, R859–R870.

AHEARN, G. A. AND ZHUANG, Z. (1996). Cellular mechanisms of calcium transport in crustaceans. *Physiol. Zool.* **69**, 383–402.

AHEARN, G. A., ZHUANG, Z., DUERR, J. AND PENNINGTON, V. (1995). Role of the invertebrate electrogenic $2Na^+/1H^+$ antiporter in monovalent and divalent cation transport. *J. exp. Biol.* **196**, 319–335.

Aiken, D. E. (1973). Proecdysis, setal development and molt prediction in American lobster, *Homarus americanus*. *J. Fish Res. Bd Can.* **30**, 1334–1337.

Bronner, F., Pansu, D. and Stein, W. D. (1986). An analysis of intestinal calcium transport across the rat intestine. *Am. J. Physiol.* **250**, G561–G569.

Davies, S., Maenz, D. D. and Cheeseman, C. I. (1987). A novel imino-acid carrier in the enterocyte basolateral membrane. *Biochim. biophys. Acta* **896**, 247–255.

Duerr, J. M. and Ahearn, G. A. (1996). Characterization of a basolateral electroneutral Na^+/H^+ antiporter in Atlantic lobster (*Homarus americanus*) hepatopancreatic epithelial vesicles. *J. exp. Biol.* **199**, 643–651.

Favus, M. (1985). Factors that influence absorption and secretion of calcium in the small intestine and colon. *Am. J. Physiol.* **248**, G147–G157.

Flik, G., *et al.* (1993). Ca^{2+} and Mg^{2+} transport in gills and gut of tilapia, *Oreochromis mossambicus*: A review. *J. exp. Zool.* **265**, 356–365.

Flik, G., Schoenmakers, T. J. M., Groot, J. A., Van Os, C. H. and Bonga, S. E. W. (1990). Calcium absorption by fish intestine: the involvement of ATP- and sodium-dependent calcium extrusion mechanisms. *J. Membrane Biol.* **113**, 13–22.

Ghijsen, W. E. J. M., Van Os, C. H., Heizmann, C. W. and Murer, H. (1986). Regulation of duodenal Ca^{2+} pump by calmodulin and vitamin D-dependent Ca^{2+}-binding protein. *Am. J. Physiol.* **251**, G223–G229.

Gunter, T. E., Gunter, K. K., Sheu, S. S. and Gavin, C. E. (1994). Mitochondrial calcium transport: physiological and pathological relevance. *Am. J. Physiol.* **267**, C313–C339.

Hildmann, B., Schmidt, A. and Murer, H. (1982). Ca^{2+} transport across basal-lateral plasma membranes from rat small intestinal epithelial cells. *J. Membr. Biol.* **65**, 55–62.

Jayakuma, A., Cheng, L., Liang, T. and Sacktor, B. (1984). Sodium gradient-dependent calcium uptake in renal basolateral membrane vesicles. *J. biol. Chem.* **259**, 10827–10833.

Kikuchi, K., Kikuchi, T. and Ghishan, F. K. (1988). Characterization of calcium transport by basolateral membrane vesicles of human small intestine. *Am. J. Physiol.* **255**, G482–G489.

Murer, H. N. and Hildmann, B. (1981). Transcellular transport of calcium and inorganic phosphate in the small intestinal epithelium. *Am. J. Physiol.* **240**, G409–G416.

Mykles, D. L. (1980). The mechanism of fluid absorption at ecdysis in the American lobster *Homarus americanus*. *J. exp. Biol.* **84**, 89–101.

Nellans, H. N. and Popovitch, J. E. (1981). Calmodulin-regulated, ATP-driven calcium transport by basolateral membranes of rat small intestine. *J. biol. Chem.* **256**, 9932–9936.

Schoenmakers, T. J. M. and Flik, G. (1992). Sodium-extruding and calcium-extruding sodium/calcium exchangers display similar calcium affinities. *J. exp. Biol.* **168**, 151–159.

Schoenmakers, T. J. M., Visser, G. J., Flik, G. and Theuvenet, A. P. R. (1992). Chelator: An improved method for computing ion concentrations in physiological solutions. *Biotechniques* **12**, 870–879.

Towle, D. W. (1993). Ion transport systems in membrane vesicles isolated from crustacean tissues. *J. exp. Zool.* **265**, 387–396.

Tsukamoto, Y., Suki, W. N., Liang, C. T. and Sacktor, B. (1986). Ca^{2+}-dependent ATPase in the basolateral membrane of rat kidney cortex. *J. biol. Chem.* **261**, 2718–2724.

Van Heeswijk, M. P. E., Geertsen, J. A. M. and Van Os, C. H. (1984). Kinetic properties of the ATP-dependent Ca^{2+} pump and the Na^+/Ca^{2+} exchange system in basolateral membranes from rat kidney cortex. *J. Membr. Biol.* **79**, 19–31.

Verbost, P. M., Schoenmakers, T. J. M., Flik, G. and Bonga, S. E. W. (1994). Kinetics of ATP- and Na^+-gradient driven Ca^{2+} transport in basolateral membranes from gills of freshwater- and seawater-adapted tilapia. *J. exp. Biol.* **186**, 95–108.

Zhuang, Z. and Ahearn, G. A. (1996). Calcium transport processes of lobster hepatopancreatic brush-border membrane vesicles. *J. exp. Biol.* **199**, 1195–1208.

Zhuang, Z., Duerr, J. M. and Ahearn, G. A. (1995). Ca^{2+} and Zn^{2+} are transported by the electrogenic $2Na^+/1H^+$ antiporter in echinoderm gastrointestinal epithelium. *J. exp. Biol.* **198**, 1207–1217.